ON DESIGN OF UNCONVENTIONAL HIGH ASPECT RATIO "JOINED-WING" TYPE AIRCRAFT

Dr. R. K. Nangia **Dr. M. E. Palmer**
Nangia Aero Research Associates,
WestPoint, 78-Queens Road, BRISTOL, BS8 1QX, UK.
Tel: +44 (0)117-987 3995 Fax: +44 (0)117-987 3995

Dr. C. P. Tilmann
Air Force Research Laboratory
Air Vehicles Directorate,
Wright-Patterson AFB, OHIO, USA
Tel: +1 937 255 4077

ABSTRACT

Unmanned Sensor Craft air vehicles have been proposed as the air-breathing component of a future intelligence, surveillance, and reconnaissance (ISR) infrastructure to provide revolutionary capabilities. Such craft must take advantage of high aspect ratio (AR) wings for aerodynamic efficiency, and may also be required to enclose an antenna in a diamond aircraft planform. A large proportion of fuel must be carried, and "loiter" is at high altitudes for a few days in each flight. This implies that a wide C_L–altitude capability is required.

This paper is concerned with aspects of configuration and design studies of high AR Sensor Craft. Implications of typical flight envelope on wing design aspects have been mentioned. Using Panel and Euler codes, results are presented for configurations with uncambered wing sections and then for configurations with designed camber and twist (trimmed for neutral stability). The designed case displays considerable reduction in LE suction, yet maintaining the lift, drag and near-elliptic wing loading characteristics. Results of an inverse design application are shown here, and further work is proposed in several areas.

1. INTRODUCTION & BACKGROUND

The Joined Wing concept conceived by Wolkovitch in 1980's (Refs.1-2) features diamond-shapes in the plan and front views. Advantage claimed was bending moment relief at a very small expense of span efficiency factor, **Figs.1-2**. Several aircraft applications were proposed (**Fig.3**). Some of the ideas were carried into experimental research aircraft and RPV. These generally had a "mixed reception" but confirmed some of the advantages claimed over "equivalent" conventional aircraft in terms of aerodynamic (large AR feasibility) and structural efficiency. There are however some adverse problems also; e.g. spanwise flows, lack of fuel volume, junction flows, etc.

With advances in technologies of controls, propulsion, and flow control, there is emphasis on re-visiting some of the older concepts and devising newer applications. Some have been publicised, **Fig.4**, e.g. Lockheed Fuel Tanker, Goldschmied (NASA), Sensor Craft etc (Refs.3-5). Some shapes feature wings joined at the tips, others part way. The tip-wings can be appropriately aft- or forward-swept.

The Air Force Research Laboratory has been formulating a program to provide revolutionary intelligence, surveillance, and reconnaissance (ISR) capabilities to the Warfighter (Ref 4). This programme blends a wide spectrum of emerging technologies to produce an unmanned air vehicle, which may be configured and optimised to conduct multiple advanced sensing modalities integrated into a single airframe that sustains an enduring theatre presence. Extremely long endurance, combined with omni-directional sensing, may enable a virtual presence, allowing vantage point flexibility / optimisation necessary for continuous and detailed theatre air and ground target detection, identification, and tracking. This unique combination of advanced sensors and sustained presence could enable continuous and rapid reaction to the dynamic combat operational requirements confronting current and evolving military operations.

The “Sensor Craft” is envisaged as the air-breather component of a fully integrated ISR enterprise that cohesively integrates space, air, and ground components of the total ISR apparatus. It is an AFRL multi-directorate shared-vision unmanned air vehicle program that combines critical vehicle, propulsion, sensor system, emerging flight and information technologies into a highly responsive platform concept to detect mobile, hidden targets. Several emerging sensor technologies are under assessment for platform use, including hyper-spectral imaging, active laser sensing, unattended ground sensors, and foliage penetration radar (Refs.5-6). **Fig.5** illustrates advanced sensor functions and modes for the Sensor-Craft.

Several candidate aircraft and propulsion configurations are under consideration to determine the best trade-off between long endurance, altitude, engine efficiency and power generation. One of the greatest challenges facing the designers is the integration of the large antenna apertures required for lower frequency operations into the airframe. These lower frequency bands of operation are required for the Sensor Craft to provide a foliage penetration radar capability, a key sensory mode aimed at defeating extremely difficult camouflaged, concealed and deceived (CC&D) targets (Ref 4)

Many of the Sensor Craft concepts take advantage of high AR wings, as well as enclosing a large antenna in a diamond aircraft planform. Such aircraft carry a large proportion of fuel and are expected to "loiter" at high altitudes for a few days in each flight. This implies a wide C_L - altitude capability, more so than existing operational reconnaissance aircraft e.g. Global Hawk. The "diamond" shapes offer useful stealth "compliance". The aerofoil shapes need to be thick for antenna and fuel tanks. The cruise Mach number is expected to be "high" subsonic. The low-speed near-field performance is more akin to that of a (very) high aspect ratio wing glider. Take-off and landing phases are demanding.

2. FLIGHT ENVELOPE, REYNOLDS NO. & CONFIGURATION CONSIDERATIONS

Previous work conducted at the AFRL indicated that the main sizing driver aspect is the integration of a "rhombic" antenna in very thick aerofoils. The payload / range performance demands lead to thick aerofoils (t/c normal to the LE, between 15 to 21%) operating at high C_L values, near 1.0.

Fig.6 gives an idea of the aircraft flight envelope. Note the Altitude and Weight relationships during a typical mission. The Reynolds number variation is also depicted as well as. Mach number and C_L relationships (C_L based on the total front wing area). Take-off is near C_L of 0.95 at Mach 0.2 (Re= 1.414×10^6/ft), whilst landing is at C_L of 0.7 at Mach 0.15 (Re= 1.06×10^6/ft). The Mach 0.6 cruise C_L varies from 1.58 to 0.88 (Re= 0.44×10^6/ft to 0.345×10^6/ft).

It is interesting to reflect that on conventional aircraft the cruise C_L values are near 0.5 and take-off / landing C_L values near 0.8 to 1.2.

The thick aerofoil sections with relative large LE radii (r) give an appreciable range of C_L or AoA operation. Predictions show "attained operation ranges (or bands)" for "attached" flow to be close to 4° in AoA.

The low and high speed design demands obviously "conflict" and this has led to a challenging effort towards suitable layouts. A previous paper for a limited audience, Ref.7, emphasised the design work using Panel codes. This paper extends the scope, using in addition, an Euler code.

3. PREDICTION METHODS

On novel layouts, often the experience is that the complexities "defy" an automatic "hands-off" design process to be used with confidence (unique solutions doubted). Therefore, we have chosen a process that allows a significant understanding to be gained with reasonable manual control over the design process (Refs.8 -18).

Panel and Euler codes are being utilised that enable assessment of the aerodynamic performance over the range of low to high speeds.

The camber and twist design, under forces and moments constraints, is via previously validated attained suction design methods (e.g. Refs.8, 9, 10, 12, 13, 15). In view of very high aspect ratios, this process has been simplified and uses a restricted set of camber and twist modes.

An inverse design method using 3-D membrane analogy (Ref.15) can "tailor" and "fine-tune" aerofoil shapes for "optimum" Cp distributions as needed.

4. DESIGN ASPECTS

At the outset, there are several aspects that need to be considered, e.g.

- Type of spanwise loadings and design of wing camber and twist.
- Trimmed flight at low speeds with different C_L levels. The TE geometry can be varied.
- High-speed design of thick wings, tolerant to a large C_L variation (fuel usage). Use of TE flaps.
- Integration of intakes / fuselages.
- "Reasonable" off-design such as cross-winds, landing / take-off.
- Roll, Pitch and Yaw Stability levels, Control laws.

We take a few of these aspects related to "high-speed" wing design in this paper. Intakes / Fuselages are not yet included.

Wing & Tail Mutual Interference

Fig.7 shows a concept outline. The front wing has continuous sweep and extends to the wing tip as shown. For early work, the wing and tail junctions are kept simple. The wing and tail are both uncambered. AoA effects can be established. Chordwise Cp distributions on both wings in dimensional and non-dimensional geometry context are shown. **Fig.8** shows the spanwise loadings with and without mutual interference. These help to highlight the tendencies for higher LE suctions towards the tip of the front wing, whilst the second wing has high LE suctions at the forward-swept centre-section. The second wing operates in the down-wash flow-field of the front wing; the largest effect occurring near the junction.

For the next part of the work, the junction has been modelled more realistically as illustrated.

Planar Uncambered Sections

Fig.9 shows the general arrangement and a 3-D perspective. This has been modelled as three wing components: front, aft and the outer tip. Also shown are uncambered aerofoil shapes.

Fig.10 shows the spanwise lift loadings arising due to AoA, on the three wing components and their sum. The forward wing is more loaded towards the wing-juncture. At the centre-line, in spite of the downwash effects, the aft wing carries more loading and this is to be expected on a forward-swept wing. For minimum drag of the total configuration, a near elliptic lift loading is required, as shown. For this layout, however, relatively high loadings appear near the wing tip.

Fig.11(a-d) shows the chordwise loadings along various wing sections at AoA = 0°, 3.25°, 4.25° and 5.25°. The corresponding C_L values are 0.0, 0.580, 0.759 and 0.936. Note the increase in LE loads as AoA increases.

At a given design condition (C_L and AoA), one could design camber and twist for minimum drag elliptic loading,but the tendency at off-design will be to depart from the elliptic loading. This will have implications on pitch trim stability.

Designed Case

The minimum C_L design point is related to landing. We have chosen C_L = 0.77 i.e. equivalent flat wing AoA of 4.25°. We have tried to approach the elliptic loading for the design. The designed case corresponds to trim for neutral stability. In view of the thick sections and anticipated attached flow band widths, the operational range should extend to C_L of 1.5.

Fig.12 shows the aerofoil design shapes compared with the uncambered case. Note the characteristic twist and camber differences for the forward-swept and aft-swept wings. The front wing has less twist/camber, compared with the rear wing.

Fig.13 shows the spanwise lift loadings due to angle of attack, on the three wing components and their sum. For minimum drag, a near elliptic lift loading is required, as shown. As AoA increases, the tips show higher loadings.

Fig.14(a-c) shows the chordwise loadings along various wing sections at AoA = 3.25°, 4.25° and 5.25°. The corresponding C_L values are 0.588, 0.768 and 0.946.

Note the upper surface flat-top nature of the chordwise pressure distributions (c.f. uncambered case, **Fig.11**). Geometry details near the wing juncture could do with some local improvements, if required. This will be more opportune at a later design stage when integrating the intakes and fuselages within the configuration.

5. PRELIMINARY COMPARISONS WITH EULER METHOD RESULTS

The main idea here was to determine, if the Panel and CFD (Unstructured Euler, Ref.19) codes gave comparable (understandable) results and to what AOA range. A secondary aim was to observe the off-design performance. The junction modeling has been kept intentionally simple for the Euler and identical results with reference to the Panel code are not expected. The CFD methods imply a very high cpu usage at subsonic speeds. In the design environment, it is often simpler and quicker to use panel codes as far as possible. Such comparative studies help in deciding the limits of applicability of the panel code. It is useful for such studies to use a near-design camber case so as to keep LE suctions reasonably "bounded".

Fig.15 compares Cp distributions for a designed wing with Panel and Euler codes. The Euler results are for C_L near 0.51 and the Panel Code results are for C_L = 0.59. The Cp and x-scales for presentation are not identical. The trends in Cp distributions are however, very similar. Note the growth of Cp near the centre-line of the aft-wing.

Fig.16 shows a sequence of Cp distributions with the Euler method as AoA is increased in 1° steps. This establishes the local "criticality" of the forward-swept root area of the second wing.

Fig.17 shows Mach number distributions for two AoA from the Euler method to support the above inference.

Further work is to be continued on this aspect. It is apparent that the Panel code can be used for design studies when LE suctions are not too large.

6. INVERSE DESIGN APPLICATION

A particular (interesting) aspect is related to adapting an Inverse Wing Design Approach With Membrane Analogy for joined wings (based on Ref.13).

To shorten time-scales for the design phase, a general 3-D approach has been devised that enables a "known" loading (target) to be "supplanted" (within reason and small tolerances) on to a wing of general planform. Aerofoil geometry, camber and twist are produced simultaneously within an iterative approach. For example, we can choose loading on a rectangular unswept wing or an elliptic planform wing as the "target".

Figs.18-20 illustrate a design exercise on the front wing of a complete joined-wing layout. **Fig.18** shows the starting situation. An unswept wing with super-critical aerofoil sections, provides the target loadings. The front (swept-back) wing loadings are generally lower than target. **Fig.19** shows the progression of loadings through 6 cycles. **Fig.20** compares the target loadings and derived loadings after 6 cycles; differences have been reduced by nearly 3/4ths. Obviously a few more cycles will achieve a closer correlation. Because the swept wing will have stagnation Cp less than 1.0 (along the span), we do not seek perfect agreement.

Fig.21 compares the aerofoil sections at start and after 6 cycles. Note the development of twist along the span.

The process described can be extended for design of front and aft wings either in turn or simultaneously. Additional constraints; stability margins, structural bending and torsion can be introduced as desired.

7. FURTHER WORK

So far, a type of Sensor Craft with a joined-wing layout has been considered for high-speed design at Mach 0.6. Several interesting features have emerged from the application of direct and inverse design methods. Further work is envisaged in a number of areas:

- Lower speeds, field performance considerations.
- Parametric geometric studies with appropriate method development.
- Different design C_L studies as required. The forward-swept root (rear wing) needs attention.
- Different aerofoils incorporation, if required, from the point of view of validation with CFD and transonic codes.
- Pitching moment, static margins control with LE / TE Flap within geometry restrictions, segmentation.
- Fuselage & Intake incorporation, additional effects on forces and moments.
- Inclusion of viscous effects, spanwise pressure gradients and flow control.
- Drag prediction.
- Off-design performance including lateral and directional characteristics.
- Include aero-elastics.
- Experimental work (various aspects).

8. CONCLUDING REMARKS

A type of Sensor Craft with a joined-wing layout has been considered for design at Mach 0.6. Several interesting features have emerged.

At the design conditions, the designed case displays considerable reductions in LE suctions when compared with the uncambered wings case. Further, near elliptic spanwise loadings have been maintained. Attention needs to be given to the forward-swept root area of the rear wing (high AoA)

Typical results presented demonstrate the flexibility and potential of the techniques towards direct and inverse design.

It is apparent that we are only at a starting post and a sizeable, interesting programme remains!

Capability for study of several geometric variables of configurations is offered in a timely sense. Data for detail design of wind tunnel models and possibly a flight demonstrator can be enabled. An understanding of control laws arises. The potential and limitations of the aircraft in meeting a given design envelope can be assessed.

Several areas for further work have emerged.

ACKNOWLEDGEMENTS

The effort is part of in-house R & D activities and also supported in part by the USAF European Office of Aerospace Research and Development (EOARD). The authors have pleasure in acknowledging helpful technical discussions with Mr. D. Multhopp, Dr. C. Jobe, Mr. W. Blake, Dr. M. OL (all from US-AFRL) & Mr. R.H. Doe (UK).

Lastly it should be mentioned that any opinions expressed are those of the authors.

REFERENCES

1. WOLKOVITCH, J., "The Joined Wing: An Overview", J. of Aircraft, Vol 23, pp. 161-178, March 1986.
2. WOLKOVITCH, J., "A Second Look at the Joined Wing", Proc. of NVVL Symposium "Unconventional Aircraft Concepts", Delft Uni. Press, 1987.
3. FREDIANI, A., "A New Large Aircraft with Box-Shaped Swept Wings", Symposium, Toulouse, 1999.
4. JOHNSON, F. P., "Sensor Craft : Tomorrow's Eyes and Ears of the Warfighter," AIAA-2001-4370, Aug. 2001. *See www.afrlhorizons.com /Briefs/Mar01/SN0001.html*
5. Aerospace America, Dec. 01, pp 50.
6. TYLER, C., SCHWABACHER & CARTER, D., "Comparison of Computational and Experimental Studies for a Joined-Wing Aircraft", AIAA 2002-0702, January 2002.

7. NANGIA, R.K., PALMER, M.E. & TILMANN, C.P., "Towards Design of Unconventional High Aspect Ratio Joined-Wing Type Aircraft Configurations", RaeS Conference – "A 2020 Vision", April 2002, London UK.

8. NANGIA, R.K., "The Design of "Manoeuvrable" Wings using Panel Methods, Attained Thrust & Euler Codes", ICAS-92.

9. NANGIA, R.K. & GREENWELL, D.I., "Wing Design of Oblique Wing Combat Aircraft", ICAS 2000-1.6.1, 2000.

10. NANGIA, R. K. & GALPIN, S.A., "Towards Design of High-Lift Krueger Flap Systems with Mach & Reynolds No. Effects for Conventional & Laminar Flow Wings", CEAS European Forum, Bath, UK, 1995.

11. NANGIA, R. K. & GALPIN, S.A., "Prediction of LE & TE Devices Aerodynamics in High-Lift Configurations with Mach & Reynolds No. Effects", ICAS-1996-2.7.6..

12 NANGIA, "Design of Conventional & Unconventional Wings for UAV's", RTA-AVT Symposium, "UV for Aerial & Naval Military Operations", Ankara, Turkey, Oct. 2000.

13 NANGIA, R.K., PALMER, M.E. & DOE, R.H., "A Study of Supersonic Aircraft with Thin Wings of Low Sweep", AIAA-2002-0709, January 2002.

14 NANGIA, R.K. & MILLER, A.S. "Vortex Flow Dilemmas & Control on Wing Planforms for High Speeds", RTO AVT Symposium, Loen, Norway, May 01.

15.NANGIA, R.K., "Developing an Inverse Design Method using 3-D Membrane Analogy", Future Paper.

16. KUCHEMANN, D. "The Aerodynamic Design of Aircraft", Pergamon.

17. JUPP, J., Wing aerodynamics and the Science of Compromise", RAeS Lanchester Lecture, 2001.

18. JONES, R.T., "Wing Theory", Princeton.

19. GUPTA, K.K. & MEEK, J.L., "Finite Element Multidisciplinary Analysis", AIAA, 2000.

NOMENCLATURE

A	= AR, Aspect Ratio
A	Axial Force along plane x-axis (definition of C_A)
b	= 2s, Wing span
c	Local Wing Chord
c_{aero}	= c, Aerodynamic wing chord
c_{av}	= c = c_{ref}, Average Wing Chord
C_A	= A/(q S), Axial Force Coefficient
C_{AL}	Local Axial Force Coefficient
C_D	= D /(q S), Drag Coefficient
C_{D0}	Drag Coefficient at zero lift (see text)
C_{Di}	Lift Induced Drag
C_L	= L/(q S), Lift Coefficient
C_{LL}	= Local Lift Coefficient
C_{Lmax}	Maximum Lift Coefficient
C_m	= m/(q S c_{av}), Pitching Moment (Body axis)
C_{m0}	C_m at zero lift
C_N	= N/(q S), Normal Force Coefficient
C_p	Coefficient of Pressure
c_r	Wing Root chord
c_t	Wing Tip chord
D	Drag force
k	= π A C_{Di}/ C_L^2, Lift Induced Drag Factor
L	Lift Force
LE	Leading Edge
LEF	Leading Edge Flap
m	Pitching moment (Body-Axis)
M	Mach Number
q	= 0.5 ρ V^2, Dynamic Pressure
r	Aerofoil radius
r_n	Aerofoil radius normal to LE
Re	Reynolds Number, usually based on c_{av}
s	Wing semi-span
S	Wing Area, (front-wing + tip-wing)
t	Aerofoil thickness
TE	Trailing Edge
TEF	Trailing Edge Flap
V	Airstream Velocity
x,y,z	Orthogonal Co-ordinates, x along bodyaxis
x_{ac}	Location of aerodynamic centre on x-axis
x_{cp}	Location of centre of pressure along x-axis
α	=AoA Angle of Attack, ref. to body-axis
λ	Taper Ratio
Λ	LE Sweep Angle
ρ	= Air Density
η	= y/s, Non-dimensional spanwise Distance

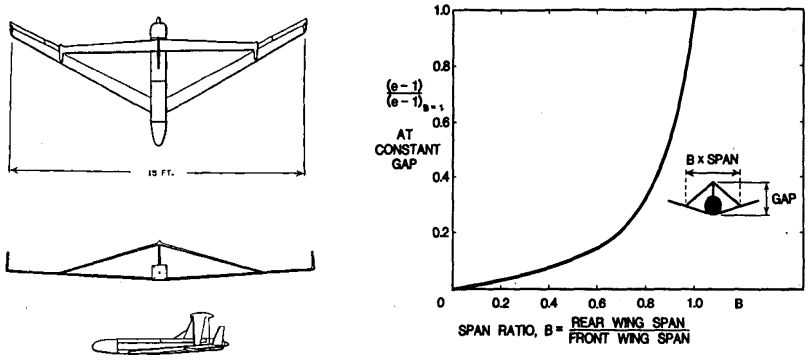

FIG.1 ACA – RPV & EFFECT OF SPAN RATIO ON SPAN EFFICIENCY

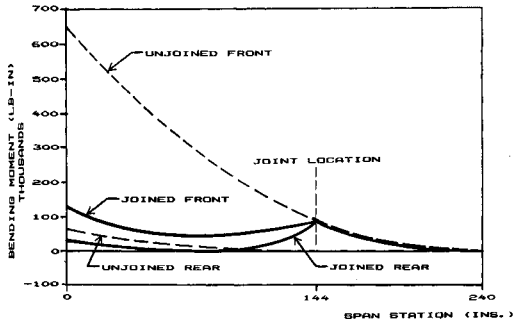

FIG.2 BENDING MOMENTS

FIG. 3 JOINED-WING CRAFT (WOLKOVITCH)

FIG. 4 SEVERAL RECENT JOINED-WING APPLICATIONS

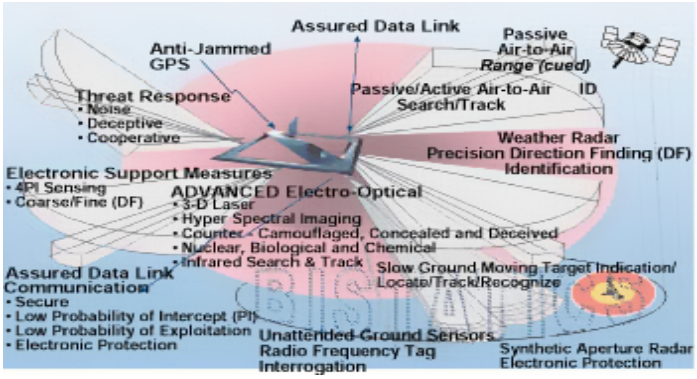

FIG. 5 SENSOR-CRAFT'S ADVANCED SENSOR MULTI-MODALITY & DIVERSE FUNCTIONALITY

FIG. 6 FLIGHT ENVELOPE, ALTITUDE - WEIGHT & CL – MACH No RELATIONSHIPS

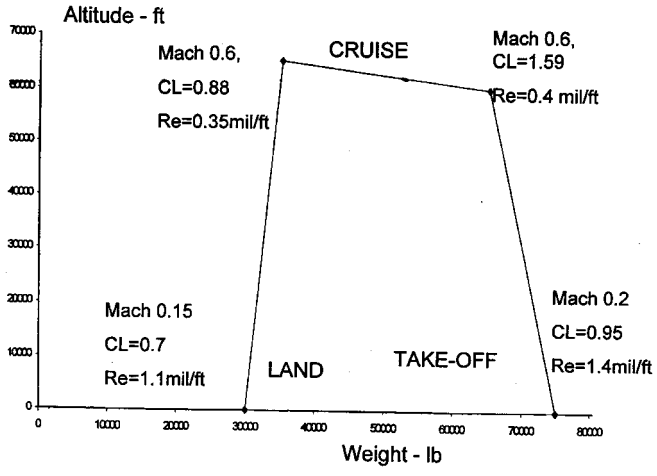

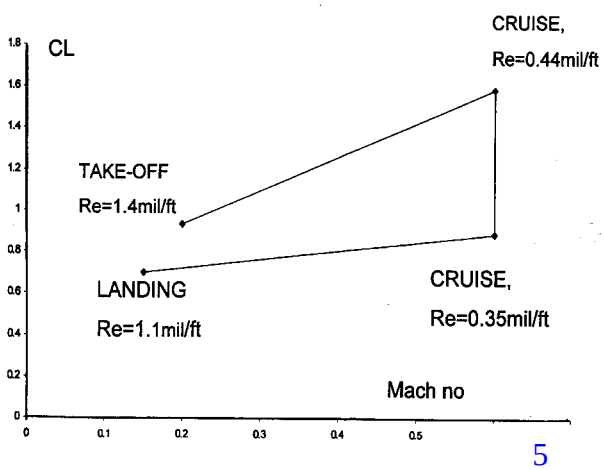

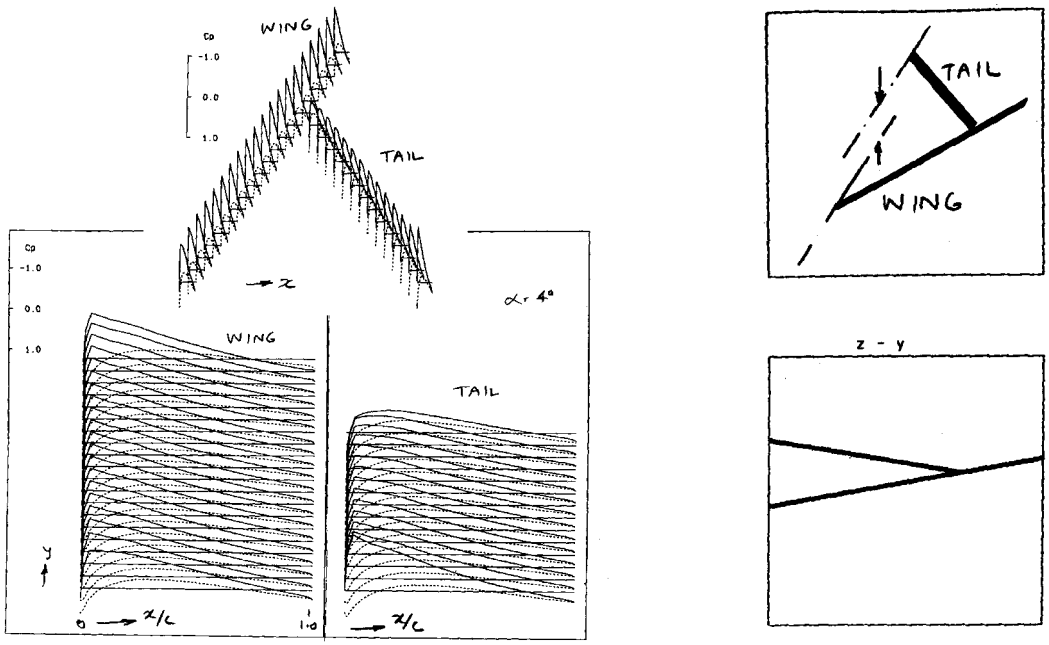

FIG. 7 JOINED-WING CONCEPT OF HIGH AR, SIMPLE JUNCTION, CHORDWISE Cp DISTRIBUTIONS, AoA=4°, SYMMETRIC AIRFOIL ON BOTH WINGS

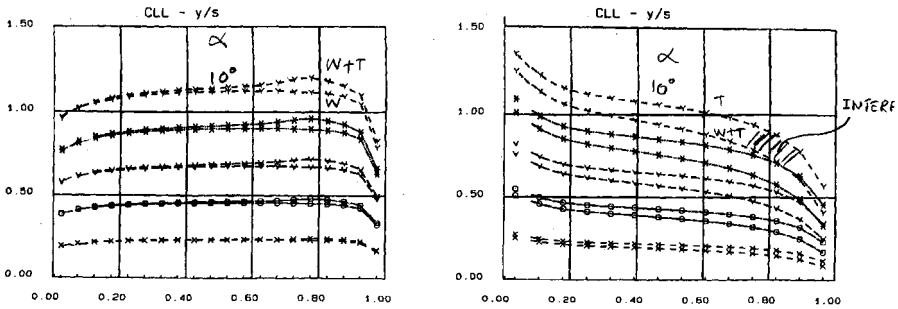

FIG. 8 SPANWISE LOADINGS WITH & WITHOUT MUTUAL INTERFERENCE

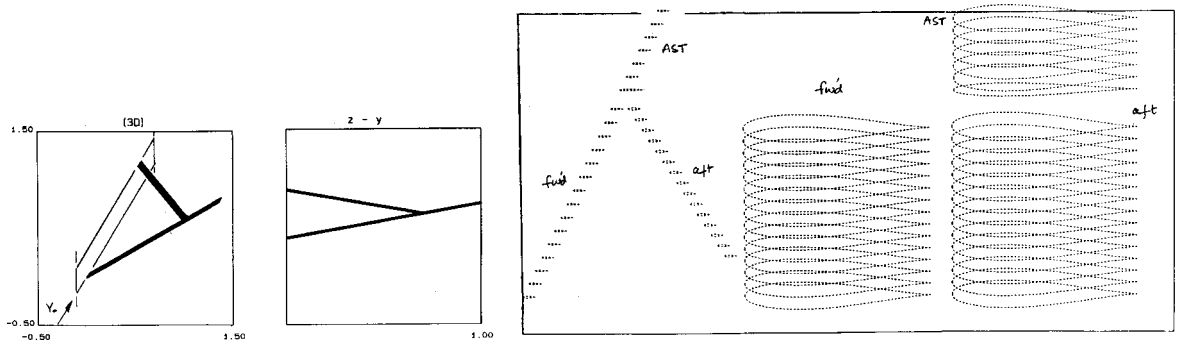

FIG.9 JOINED-WING CONCEPT WITH MORE DETAILED JUNCTION MODELLING & UNCAMBERED AIRFOIL SHAPES

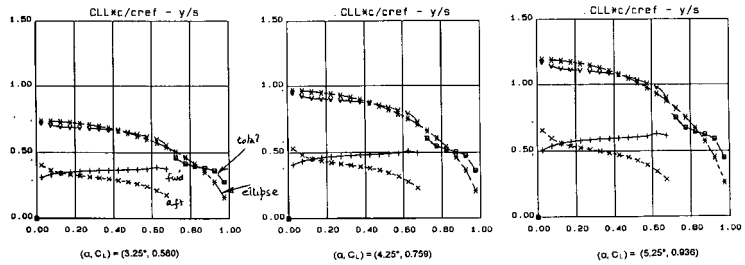

Fig.10 UNCAMBERED WINGS, C_{LL} SPANWISE LOADINGS AT 3 C_L

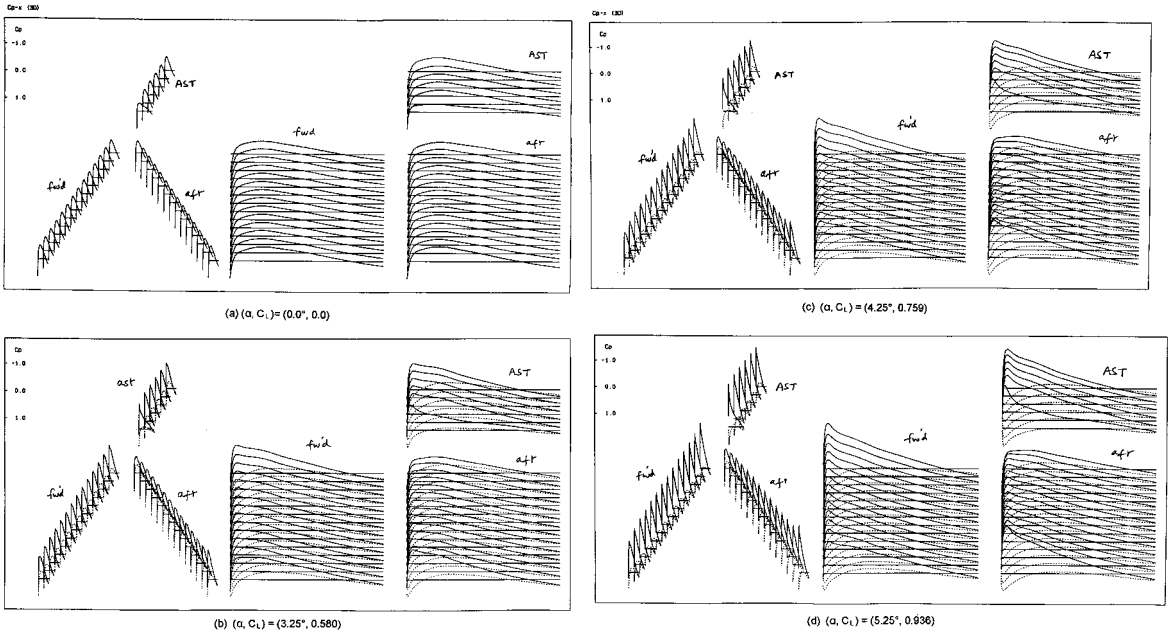

FIG. 11 UNCAMBERED WINGS, Cp DISTRIBUTIONS

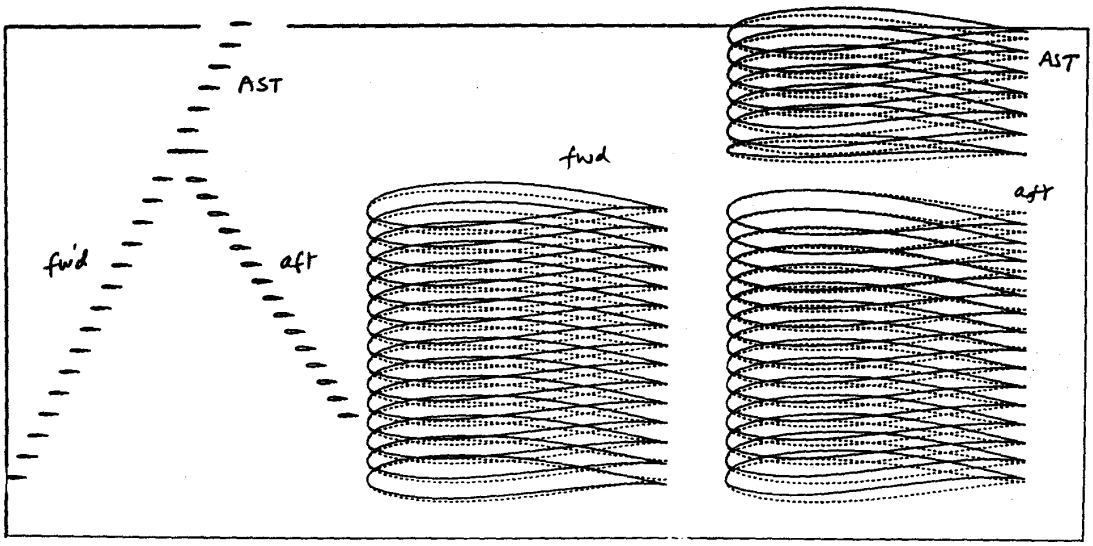

FIG. 12 DESIGNED CONFIGURATION, AIRFOIL SHAPES

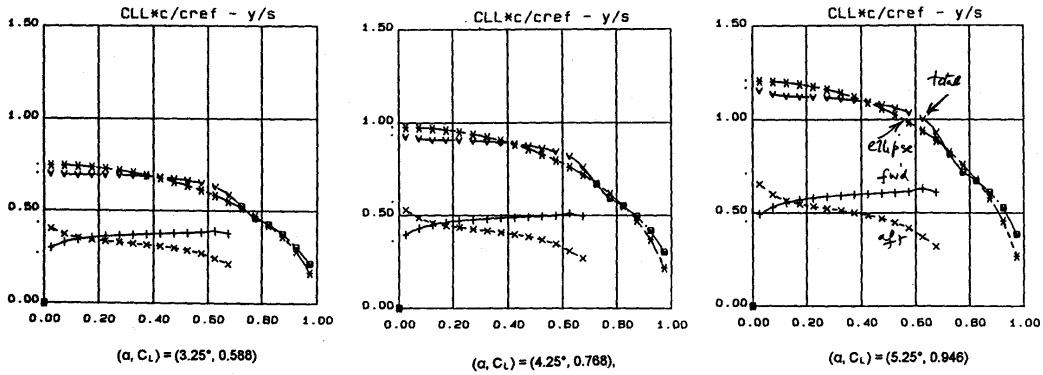

FIG.13 DESIGNED WINGS, C_{LL} SPANWISE LOADING

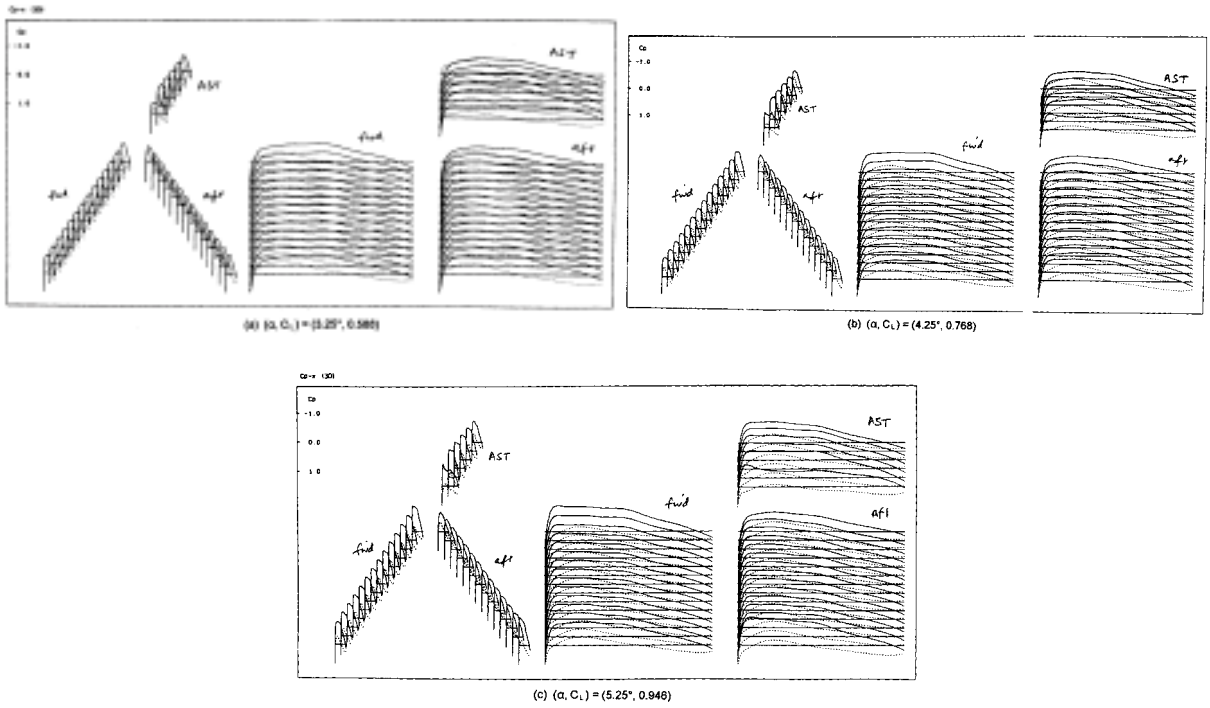

FIG. 14 DESIGNED WINGS, C_P DISTRIBUTIONS

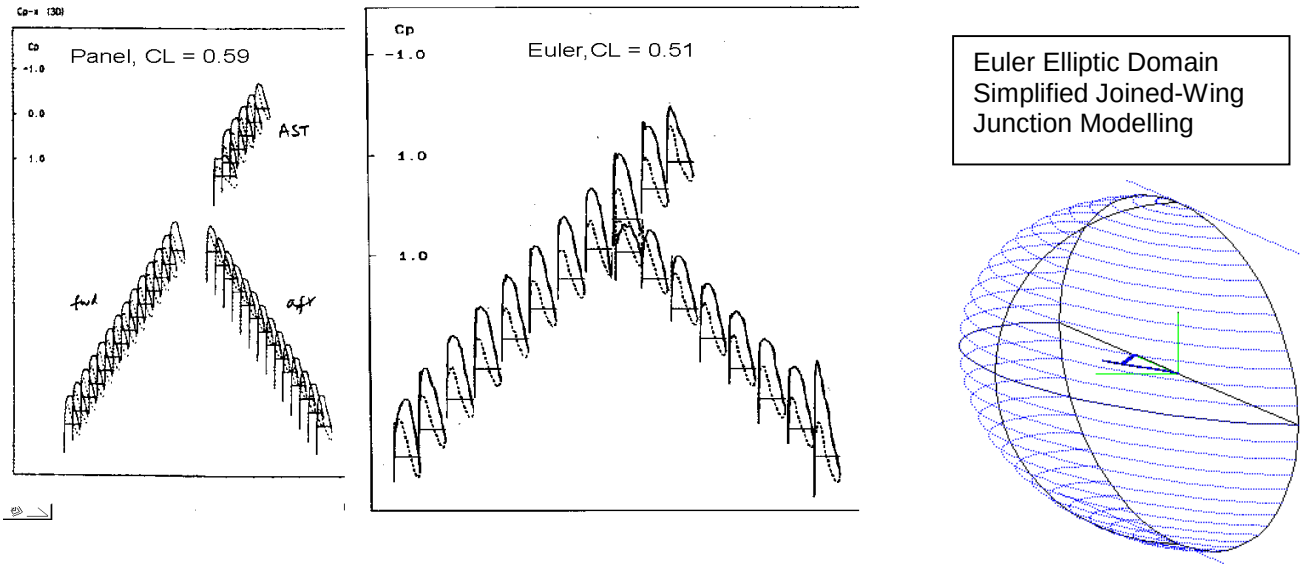

FIG. 15 DESIGN CASE, RELATING PANEL & EULER Cp DISTRIBUTIONS
Note: At Present, the Euler Modelling is for a simple Junction

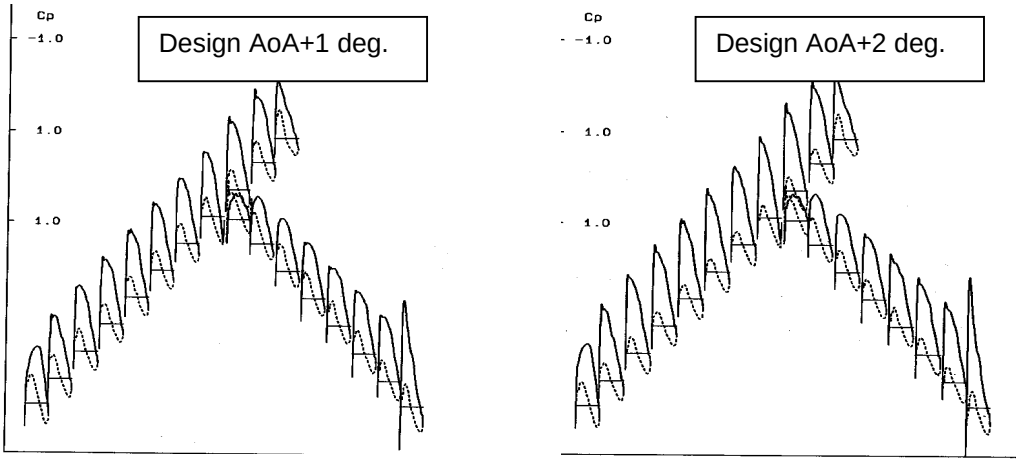

FIG. 16
See also overleaf

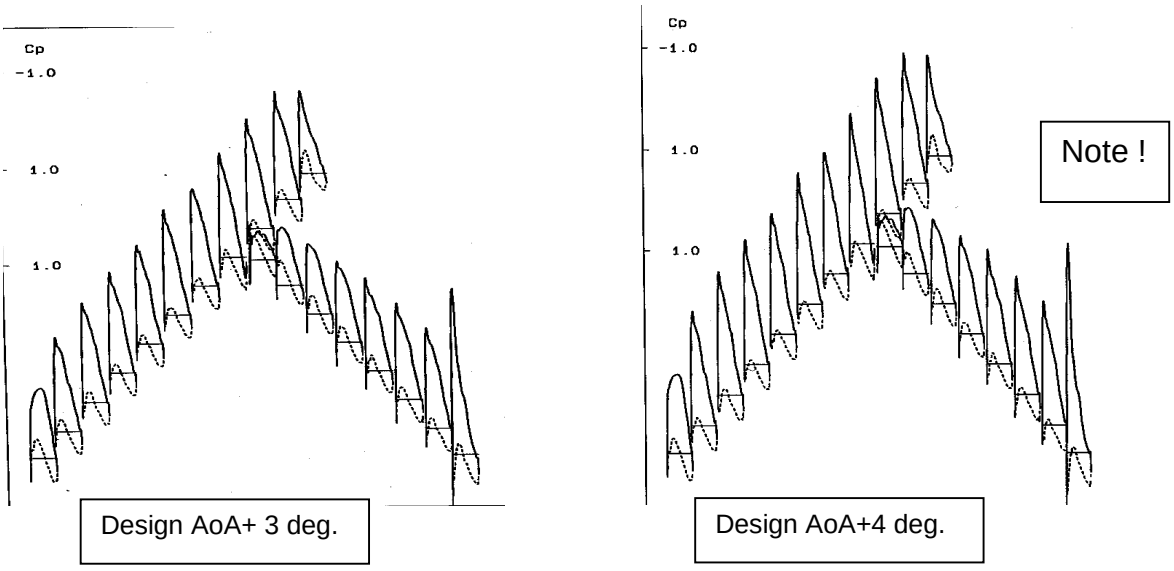

FIG. 16 Cp DISTRIBUTIONS FROM EULER

Upper Surface

Lower Surface

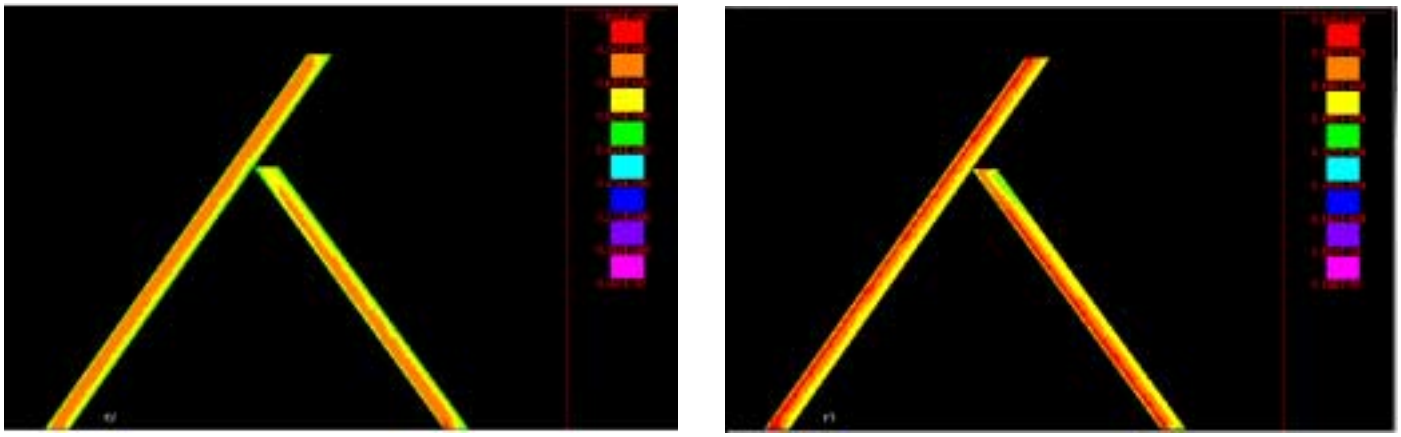

Design AoA + 0 deg.

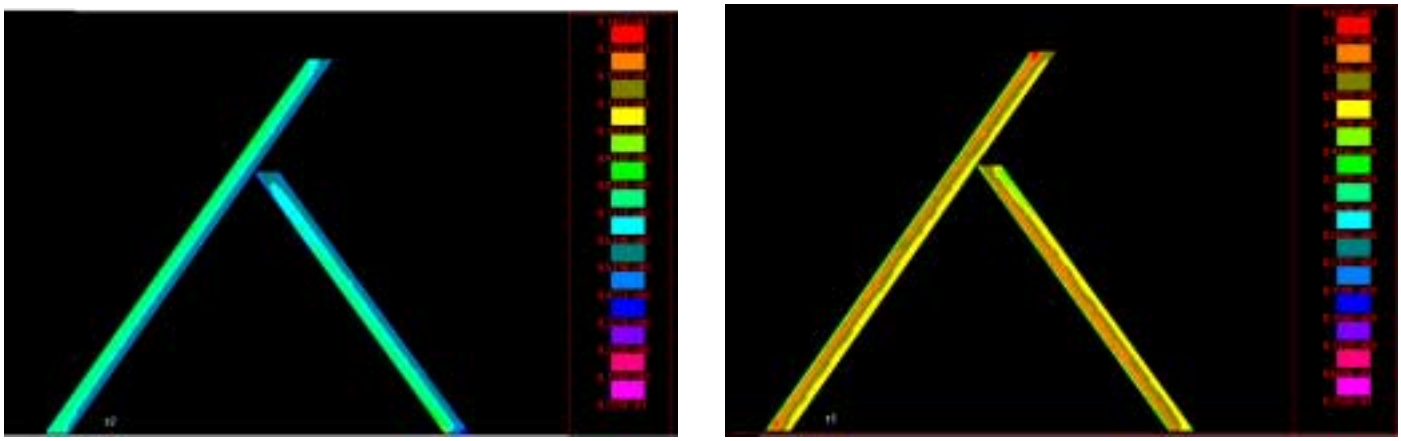

Design AoA + 4 deg.

FIG. 17 MACH No DISTRIBUTIONS FROM EULER

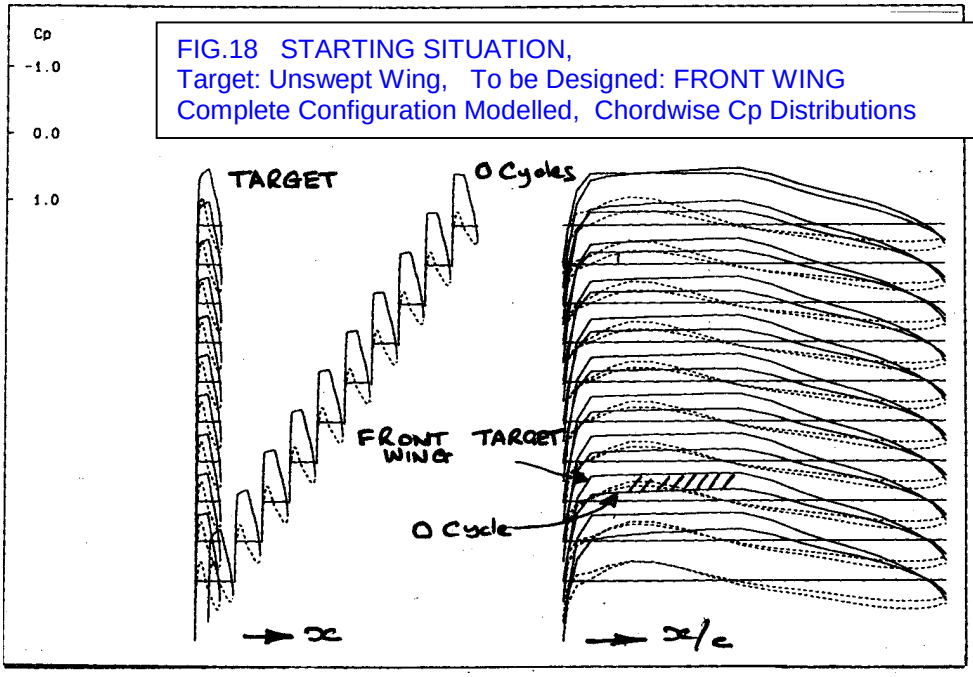

FIG.18 STARTING SITUATION,
Target: Unswept Wing, To be Designed: FRONT WING
Complete Configuration Modelled, Chordwise Cp Distributions

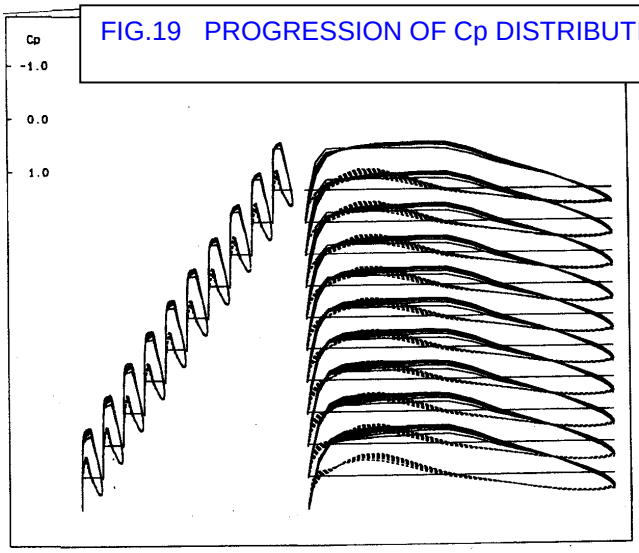

FIG.19 PROGRESSION OF Cp DISTRIBUTIONS THROUGH 6 CYCLES

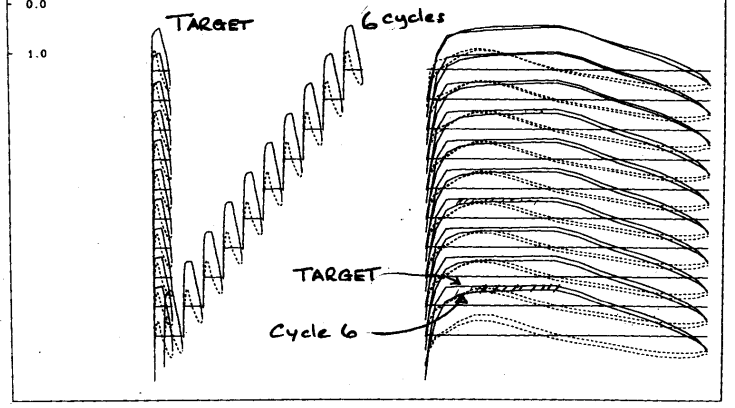

FIG. 20 COMPARING Cp DISTBNS.
TARGET & FRONT WING AFTER 6 CYCLES

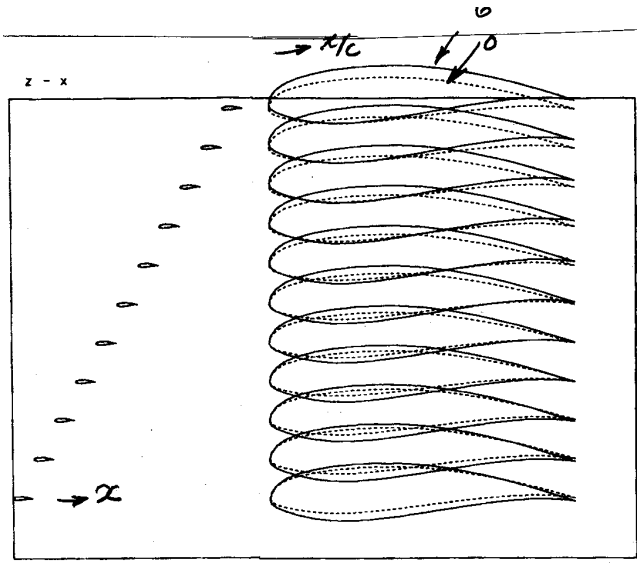

FIG. 21 COMPARING AEROFOIL SECTIONS
AT START & AFTER 6 CYCLES
COMPLETE CONFIG. MODELLED